Physics – Uspekhi **67** (10) 1022 – 1033 (2024)

REVIEWS OF TOPICAL PROBLEMS PACS numbers: **05.70. – a,** 64.70.D – , **65.40. – b**

Thermodynamic properties of zirconium nitride in the condensed state

N M Aristova, S V Onufriev, A I Savvatimskiy

DOI: https://doi.org/10.3367/UFNe.2024.02.039654

Contents

Abstract. The thermodynamic properties of zirconium nitride are presented, including the phase diagram of the Zr–N system, homogeneity region, temperature and composition corresponding to congruent melting of ZrN_x, enthalpy of formation, as well as electronic structure and chemical bond in zirconium nitride. An equation is given approximating the temperature dependence of the heat capacity of crystalline ZrN in the temperature range of 298.15–3970 K. Temperature dependences of specific heat and electrical resistance of liquid zirconium nitride of the composition $0.9ZrN + 0.1ZrO_2$ (up to 4500 K) measured by heating with a microsecond current pulse are presented. The main practical significance of these results is that ZrN serves as an inert matrix for mixed nitride fuel (U, Zr)N and (Pu, Zr)N for fast neutron reactors.

Keywords: nuclear fuel matrices, zirconium nitride, phase diagrams, solid phases, melting, liquid state, enthalpy of formation, enthalpy, specific heat, electrical resistance, temperature measurement, pulsed current heating method

1. Introduction

Zirconium mononitride ZrN has a number of unique physical, chemical, thermal, and mechanical properties, which determines its use in modern technologies and makes it a promising material for future technologies.

Zirconium nitride has a high melting point, high electrical and thermal conductivity, relatively high emissive capacity in the visible and near IR regions, good resistance to acid and alkali solutions, high hardness and wear resistance, and good mechanical properties. Among metal nitrides and carbides, its superconducting transition temperature of ~ 10 K is the second highest after that in niobium nitride. Zirconium nitride is used in power engineering, in particular nuclear energy, aviation, and rocket and space technology.

This review covers the following topics.

(1) Critical analysis of published data (1930–2020) on the solid state of ZrN:

— phase diagram;
— melting point;
— enthalpy of formation;
— electronic structure and chemical bonding;
— superconductivity;
— low-temperature heat capacity;
— high-temperature enthalpy and heat capacity (solid state).

(2) Equation approximating the temperature dependence of the heat capacity of ZrN in the range of 298.15–3970 K.

(3) Experimental data for $0.9\,ZrN + 0.1\,ZrO_2$ (specific heat capacity and electrical resistance) during melting and in the liquid state (up to 4000 K).

(4) Application of zirconium nitride and prospects for using the method of heating substances with a short current pulse for the purpose of measuring high-temperature physical properties of materials used in nuclear power and other technical applications.

The need for such an analysis is due to the development of nuclear technologies and particularly the prospects for using nitride fuels.

Nitride fuel research and development programs for fast neutron reactors (Generation IV) were launched in the

N M Aristova [1, a], **S V Onufriev** [1, b], **A I Savvatimskiy** [1, 2, c]
[1] Joint Institute for High Temperatures, Russian Academy of Sciences, ul. Izhorskaya 13, str. 2, 125412 Moscow, Russian Federation
[5] Lebedev Physical Institute, Russian Academy of Sciences, Leninskii prosp. 53, 119991 Moscow, Russian Federation
E-mail: [a] aristo2012@yandex.ru, [b] s-onufriev@yandex.ru, [c] savvatimskiy.alexander@gmail.com

Received 4 October 2023, revised 28 January 2024
Uspekhi Fizicheskikh Nauk **194** (10) 1082 – 1094 (2024)
Translated by V L Derbov

United States, France, Germany, the United Kingdom, Russia, Japan, and India back in the 1960s and 1970s. The resumption and continuation of international programs to create fourth-generation reactors has been reflected in the work of international forums [1–3].

Sustainable development of nuclear energy requires the creation of advanced fast breeder reactors. As international initiatives related to Generation IV reactors have shown, there remains a pressing need for better fuel characteristics for this class of reactors, maintaining the integrity of the rods at high temperatures, achieving the highest possible burnup, as well as the subsequent regeneration of spent fuel and use of structural systems [4].

In 2011, the state program Proryv (Breakthrough) of the Rosatom State Corporation was launched. Mixed nitride uranium-plutonium fuel (MNUPF) (U, Pu)N is considered the basis for future fast closed-cycle power reactors, particularly those such as BREST-300 and BN-1200. Closing the nuclear fuel cycle and developing reactors with expanded fuel breeding are considered to be some of the innovative development of nuclear energy.

The advantages of nitride fuel (U, Pu)N over oxide fuel are well known: it has a higher density and thermal conductivity, the yield of aggressive fission products (cesium, iodine, selenium, tellurium, etc.) is significantly less than from oxide fuel, and, as a result, there is less corrosion of the cladding of fuel elements [5–8]. Fuel elements with dense nitride uranium-plutonium fuel are an innovative development implemented in Russia. However, some unexpected difficulties arose in the process of developing technologies for creating this new type of fuel. A whole series of experimental and computational studies performed at the Kurchatov Institute National Research Center [9–12] are devoted to clarifying the reasons for the degradation of the mechanical characteristics of steel claddings and fuel elements during interaction with (U, Pu)N fuel and developing methods for eliminating undesirable effects. Thermodynamic analysis and calculations of the equilibrium chemical and phase composition of the fuel, presented in this work, were performed using the IVTANTERMO software package developed at the Joint Institute for High Temperatures of the Russian Academy of Sciences.

Of particular interest is the effect of carbon and oxygen impurities on the phase and chemical composition of the fuel during its irradiation and on the mechanical characteristics of the steel cladding of the fuel elements. The research results presented in [13] indicate that the presence of oxygen impurities significantly affects the physicochemical properties of the fuel. In particular, the presence of 1 wt.% oxygen reduces the thermal conductivity of the fuel by 9–13%. Carbon present in the initial nitride fuel as an impurity, as well as carbon produced during burnout, worsens the mechanical properties of steel fuel elements in the contact zones with the fuel compared to fuel elements in contact with oxide fuel.

Another type of mixed nitride, such as (U, Zr)N and (Pu, Zr)N, is currently considered a possible nuclear fuel for high-temperature reactors. In this case, zirconium nitride serves as an inert matrix [14, 15]. The crystal structure, microstructure, and density of zirconium nitride ZrN samples obtained by spark plasma sintering and used in nuclear inert matrix fuel (IMF) were studied in [15].

It is obvious that the inert matrix material of nitride fuel must have a number of properties, such as a high melting point, thermal conductivity, hardness, and radiation stability. Zirconium nitride is fully endowed with all these properties, due to which it is especially attractive for use both in modern nuclear power plants and as an ultra-high-temperature ceramic for other applications in extreme environments.

One of the problems limiting the use of this type of fuel is its insufficient study. To obtain comprehensive knowledge of nitride fuel systems, it is necessary to create a reliable and complete database that will allow, based on experimental and theoretical work, improving and developing the necessary modeling tools for predicting the behavior of modern fuels in the reactor core.

Reviews and critical analysis of all available information in the literature on the thermodynamic properties of zirconium nitride in the condensed state and calculations performed on their basis make it possible to model high-temperature processes in a nuclear reactor containing ZrN_x.

2. Phase diagram of Zr–N system

The phase diagram of a binary Zr–N system has been investigated in many experimental and computing studies; it is also reflected in reviews and reference books [16–36].

The base equilibrium phase diagram of the Zr–N system at a pressure of 1 atm [28] is shown in Fig. 1. The authors of [28] used the experimental data obtained in [16–18, 23] when calculating the diagram. The Zr–N phase diagram includes: (1) the nonstoichiometric phase ZrN_x with an NaCl face-centered cubic (FCC) structure, which is stable in the composition series from ~ 40 to 50 at.% of N; (2) a solid solution of nitrogen in zirconium with a hexagonal close-packed (HCP) structure (αZr); (3) a solid solution of nitrogen in body-centered cubic (BCC) zirconium (βZr); (4) a liquid phase (L); 5) a gas phase (G).

The stability region of ZrN_x in the equilibrium phase diagram is determined by its coexistence with solid solution (αZr), liquid (L), and gas (G) phases. The ZrN_x phase has a wide range of nonstoichiometry associated with the formation of vacancies in the nitrogen sublattice. According to Ref. [25], ZrN_x exists in a compositional series from $ZrN_{0.63}$ to $ZrN_{1.00}$ and can accumulate up to 35% of vacant positions in the nitrogen sublattice. The composition of 50 at.% of N corresponds to the complete filling of the octahedral sites (positions) in the NaCl structure with nitrogen atoms. The

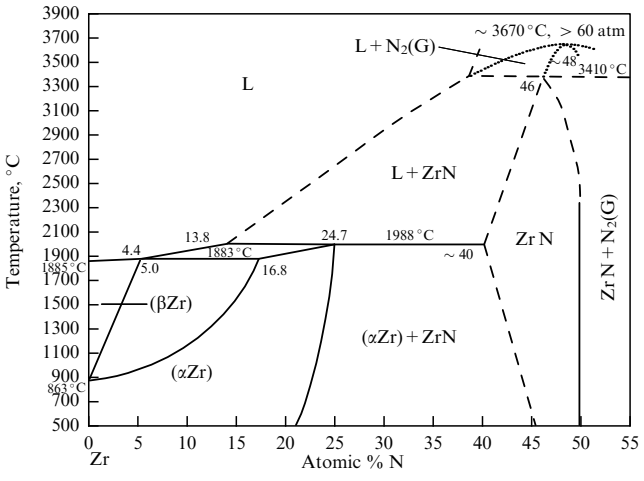

Figure 1. Phase diagram of Zr–N system [28].

limits of the homogeneity region depend on the method of obtaining the nitride, nitrogen pressure, the presence of impurities, etc. According to [21], the mononitride phase is stable in the series of compositions from $ZrN_{0.6}$ to ZrN at 2258 K. In [17, 18], equilibria in the Zr–N system were studied in the temperature range of 2100–2800 K at nitrogen pressures of 0.1–300 mm Hg. As a result of the study, various equilibrium compositions of zirconium nitride were obtained in the range of $ZrN_{0.56}$–$ZrN_{0.97}$. According to the authors of [17], the composition $ZrN_{1.0}$ should be considered a rarely realized case. To obtain it, higher pressure and a longer time are probably required. It was noted that, in the process of approaching the stoichiometric composition, the color of the nitride changes from grayish yellow to golden.

As data on the structural, thermophysical, and thermodynamic properties of zirconium nitride accumulated, the basic phase diagram of the Zr–N system [28] was supplemented or partially revised in [29, 30, 32, 35].

The author of [29] assessed the structure and stability of the (αZr) and (βZr) phases, as well as the part of the Zr–N phase diagram rich in zirconium.

The authors of [30] assessed the thermodynamic functions of the Zr–N system in the temperature range of 1500–3670 K. The pressure-composition-temperature relationships were determined in the poorly studied regions of (βZr) and $Zr(L)/ZrN_c$. The Gibbs energies of a nitrogen solution in solid and liquid zirconium were calculated.

Optimization of the thermodynamic parameters of the Zr–N phase diagram using the CALPHAD method was performed in [32]. A complete $T-x$ phase diagram for the binary Zr–N system at temperatures above 500 K and a pressure of 1 atm is presented based on available experimental data and the results of calculations using the density functional theory (DFT).

When considering the nonstoichiometric phase of ZrN_x, a sublattice model with the introduction of nitrogen vacancies $Zr_1(N, Va)_1$ was used. According to the obtained phase diagram, shown in Fig. 2, zirconium mononitride ZrN_x is stable in the series of compositions from 38.1 to 50 at. % of N at a temperature of 2272 K.

The melting point of ZrN_x at a nitrogen pressure of 1 atm is 3084 K and corresponds to a composition of 46.5 at.% of N. Comparing the Zr–N phase diagram calculated by the CALPHAD method [32] with the basic one [28] shows good agreement of the data regarding the maximum homogeneity region of ZrN_x, which, according to [28], is ~ 40–50 at.% of N at a temperature of 2261 ± 16 K. As for the melting point of ZrN_x, a significant discrepancy should be noted here: according to [28], $T_m = 3683$ K at a nitrogen pressure of 1 atm and corresponds to a composition of 46 at.% of N. Such a significant discrepancy in the melting point values can be explained by the different choice and preference of studies devoted to the determination of T_m.

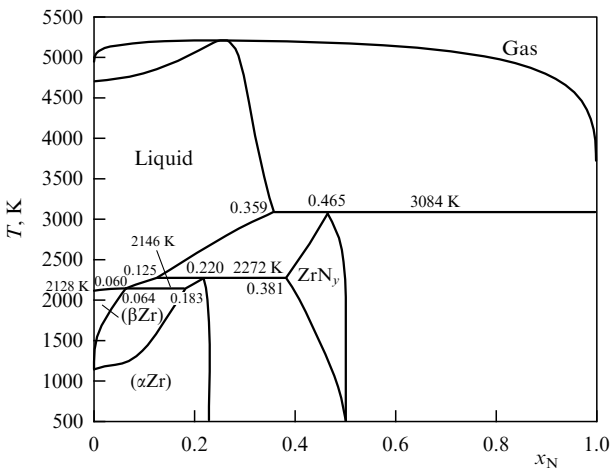

Figure 2. Phase diagram of Zr–N system calculated by CALPHAD method [32].

Thermodynamic modeling of the Zr–N system using the CALPHAD method associated with *ab initio* calculations was undertaken in Ref. [35]. The authors used all experimental, crystallographic, structural, and thermochemical data available in the literature for the equilibrium phases in this system. As a result of the calculations, the thermodynamic parameters of the (αZr), (βZr), and ZrN phases, as well as the liquid phase (L), were obtained.

3. ZrN_x melting temperature

The temperature and stoichiometry of the ZrN_x composition, corresponding to the congruent nature of melting, are still the subject of research and discussion. The melting point of zirconium nitride has been determined in experimental [23, 37–42] and computational studies [28, 29, 32]. It is known that T_m of transition metal nitrides depends significantly on the equilibrium nitrogen pressure. In this regard, the authors of [23, 40, 42] investigated the effect of nitrogen pressure on the melting point of nonstoichiometric ZrN_x in the homogeneity region ($ZrN_{0.85}$–$ZrN_{0.98}$). The studies were carried out in a sealed water-cooled chamber in the pressure range of $10^{-3}-60$ atm and at temperatures of 2753–3973 K. The nitrogen pressure, measured by manometers of different types, was determined with an accuracy of ±1%. The error in temperature measurements using an optical pyrometer is estimated at ±1%. ZrN_x samples were obtained by nitriding zirconium foil with 99.999% pure nitrogen. Equilibrium preparations were obtained by isothermal holdings of zirconium nitride at a certain nitrogen pressure until a constant composition was achieved.

In Ref. [23], it was found that, at a nitrogen pressure of 60 atm, zirconium nitride melts congruently at a temperature of 3970 ± 70 K, while its composition corresponds to the formula $ZrN_{0.98}$. The obtained melting point value is more than ~ 700 K higher than the values of T_m given in earlier papers [37] (3200 ± 50 K), [38] (3255 ± 50 K), and [39] (3283 K). In the listed studies, melting point measurements were performed at a nitrogen pressure of 1 atm. In addition, according to the analysis, the sample used in Ref. [37] contained an oxygen impurity in the form of 7.5 wt.% of ZrO_2. It was shown that the oxygen impurity significantly (by 200–300 degrees) lowers the melting point of zirconium nitride.

A study of the dependence of the melting point of ZrN_x on the nitrogen pressure under conditions of thermal equilibrium between the gas and the nitride surface showed that, at nitrogen pressures of 0.1, 1, 10, and 60 atm, the melting points are 3333, 3523, 3733, and 3973 K, respectively [42]. In this case, the compositions of the solid phase and the solid phase in equilibrium with the liquid were close to each other only in samples melted at a nitrogen pressure of 60 atm or higher. In other cases, they differed significantly, indicating an incongruent nature of melting.

In addition to experimental work, the melting behavior of ZrN_x was investigated using calculations [28, 29, 32].

According to thermodynamic calculations [28], based on experimental data, ZrN_x melts congruently at a temperature of $\sim$ 3943 K and a composition of 48 at.% of N (nitrogen pressure is higher than 60 atm). It was also found that, at a nitrogen pressure of 1 atm, ZrN_x melts incongruently at 3683 K and 46 at.% of N. According to the results of thermodynamic modeling in [29], the competitive melting temperature of zirconium nitride is 3233 K and corresponds to the stoichiometric composition ZrN (50 at.% of N). According to [32], the melting temperature of ZrN_x at a nitrogen pressure of 1 atm is 3084 K and corresponds to a composition of 46.5 at.% of N.

Obviously, with such a spread of data on the temperature and composition of ZrN_x corresponding to the competitive nature of melting, further direct experimental studies are necessary, as is numerical modeling based on a critical assessment of the entire array of experimental data.

In this paper, preference is given to studies [23, 42]: zirconium nitride melts specifically at a temperature of 3970 ± 70 K, while its composition corresponds to the formula $ZrN_{0.98}$. When choosing the value of T_m, the quality of the samples was taken into account, confirmed by X-ray and chemical analysis, as well as the thoroughness in conducting the experiment.

4. ZrN_x formation enthalpy

The enthalpy of zirconium nitride formation was determined by the calorimetric method in [43, 44]. The preparations used in [43] were obtained by nitriding zirconium powder in a nitrogen stream at 1373 K. The samples contained 12.09–12.245 wt.% of nitrogen, which corresponds to a nitride frequency of 90.86–91.99%. The combustion of the samples in oxygen in a calorimetric bomb was carried out at an oxygen pressure of 25 atm. For the enthalpy of formation of ZrN (cr.) at 292 K, the authors of [43] obtained a value of -343.9 kJ mol^{-1}.

A more reliable value for the formation enthalpy of zirconium mononitride, close in composition to stoichiometric, was obtained in Ref. [44]. Two batches of samples were prepared by nitriding zirconium in a stream of high-purity nitrogen for 5 h at 1300–1400 K. According to X-ray and chemical analyses, both batches of samples were single-phase and contained 13.35 (batch A) and 13.31 (batch B) wt.% of nitrogen with a theoretical content of 13.31 wt.% of N. The samples were burned in oxygen (30 atm) at 303.15 K. According to [44], the combustion completeness of samples from batch A was 99.95%, and that of preparations from batch B was 99.956%. Based on the enthalpy of formation of $\Delta_f H^0$ (ZrO_2, cr., 298.16 K) $= -1094.1 \pm 0.8$ kJ mol^{-1} [45], the authors of [44] obtained the value of -365.3 ± 1.7 kJ mol^{-1} for the standard enthalpy of ZrN (cr.) formation at 298.15 K.

The evaporation of ZrN at temperatures of 2236–2466 K was studied by the Knudsen effusion method in Ref. [46]. According to the authors, during evaporation, ZrN decomposes into metallic Zr and nitrogen N_2. Considering the enthalpy of this reaction (332.8 kJ mol^{-1}), the standard enthalpy of formation of $\Delta_f H^0$ (298 K) $= -336.5$ kJ mol^{-1} for ZrN was calculated.

In Ref. [47], based on measurements of the thermal effect of explosion of a mixture of lead azide in zirconium ($PbN_6 + Zr$), the value of -301 kJ mol^{-1} was obtained for the enthalpy of zirconium nitride formation at 298 K. Experiments with mixtures were carried out in a calorimetric bomb made of stainless steel. The content of powdered zirconium in the mixture was 65.2 wt.%. The error in measuring the thermal effect of explosion did not exceed 0.4%.

The enthalpy of ZrN_x formation in the homogeneity region and of a solid solution of nitrogen in zirconium (α-phase) were determined by the calorimetric method in [18, 48, 49]. The starting materials for obtaining zirconium nitrides of various compositions from $ZrN_{0.56}$ to $ZrN_{0.97}$ [18, 48] were metallic zirconium of 99.7 purity, special purity nitrogen, or purified ammonia. According to chemical and X-ray phase analysis, all compositions have a face-centered cubic lattice. The combustion products of zirconium nitride and a solid solution of any composition are ZrO_2 and nitrogen. The standard enthalpy of ZrO_2 (cr.) formation (-1100.6 ± 0.7 kJ mol^{-1}) required for calculations was taken from [50]. It should be noted that the value of $\Delta_f H^0$ (ZrO_2, cr., 298.16 K) obtained in [50] is in excellent agreement with the value of the corresponding quantity obtained earlier in Ref. [45]. As established by the authors of Refs [18, 48], with a change in the composition of ZrN_x ($x = 0.56-0.97$), the enthalpies of ZrN_x formation change significantly (from -234.7 ± 2.9 kJ mol^{-1} to -367.8 ± 0.8 kJ mol^{-1} at 298 K), which should be taken into account in thermodynamic calculations.

In Ref. [49], samples of a solid solution of nitrogen in zirconium (α-phase) were prepared by sintering a thoroughly ground mixture of zirconium nitride of the composition $ZrN_{0.85}$ with metallic zirconium. Subsequent annealing was carried out in a nitrogen atmosphere at a temperature of 1000 °C for 500 h. The dependence of the formation enthalpy of a solid solution of nitrogen in zirconium and zirconium nitride on the composition in the homogeneity region are approximated by two expressions ((1) and (2), respectively):

$$\Delta_f H^0 (ZrN_x, 298\ \text{K}) = -429.3x \pm 7.1\ [\text{kJ mol}^{-1}] \quad (0 < x \leqslant 0.78), \tag{1}$$

$$\Delta_f H^0 (ZrN_x, 298\ \text{K}) = -(202.1 + 169.5x) \pm 9.2\ [\text{kJ mol}^{-1}]\ (0.78 \leqslant x \leqslant 1). \tag{2}$$

According to Eqn (2), for stoichiometric zirconium nitride $\Delta_f H^0$(ZrN, 298 K) $= -371.6 \pm 9.2$ kJ mol^{-1}.

Along with experimental determinations of the zirconium nitride formation enthalpy, this value was estimated using various calculation methods in Refs [30, 32, 35, 51].

The authors of Ref. [30] estimated the formation enthalpy of zirconium nitride $\Delta_f H^0$ (ZrN) $= -370$ kJ mol^{-1} at 298 K and established a relationship between the heat of nitride formation and the N/Zr ratio.

The enthalpies of formation of stoichiometric nitrides and carbides of transition metals, including zirconium nitride, were estimated in Ref. [51] using the chemical bond model. The bond model is based on the interaction between the d-orbitals of the metal and the p-orbitals of the nonmetal in compounds that crystallize in the NaCl structure. For stoichiometric ZrN, the calculated value of the formation enthalpy was $\Delta_f H^0$ (298 K) $= -365.3$ kJ mol^{-1}.

Using the local density approximation (LDA) and generalized gradient approximation (GGA) methods, the authors of [32] estimated the enthalpy of stoichiometric ZrN formation as -332.897 and -416.599 kJ mol^{-1}, respectively.

In Ref. [35], thermodynamic modeling of the solid phase in the Zr–N system was performed using the CALPHAD method in comparison with *ab initio* calculations. Based on the analysis of all experimental data available in the literature, obtained during thermochemical and thermophysical studies, the authors of Ref. [35] calculated various thermodynamic parameters, including the enthalpy of stoichiometric zirconium nitride formation: $\Delta_f H^0$ (ZrN, 298 K) = −350.444 kJ mol^{-1} (CALPHAD); $\Delta_f H^0$ (ZrN, 298 K) = −341.593 kJ mol^{-1} (*ab initio*).

Based on an analysis of the entire set of data presented above, for practical calculations, it is possible to recommend the value of the formation enthalpy of zirconium mononitrides (stoichiometric and nitrogen-defective), obtained experimentally in Refs [18, 44, 49]. For stoichiometric zirconium nitride ZrN, the following consistent values are given: $\Delta_f H^0$ (298 K) = −367.8 ± 0.8 kJ mol^{-1} [18], −365.3± 1.7 kJ mol^{-1} [37], −371.6 ± 9.2 kJ mol^{-1} [49]. The average value of the enthalpy of formation for stoichiometric zirconium nitride, taking into account the weights of the given values equal to $1/(\Delta i)^2$ (where Δi is the uncertainty of the ith value), is $\Delta_f H^0$ (298 K) ≈ −366.98 ± 1.00 kJ mol^{-1}.

5. Electronic structure. Chemical bond

The electronic structure and nature of the chemical bond in zirconium nitride are considered in Refs [21, 31, 34, 52–58], based on numerous experimental studies and calculated data. An analysis of the papers showed that the chemical bond in nitrides of transition metals of group IV has a complex nature and includes contributions from covalent, metallic, and ionic components. Due to this combination of bonds, the materials have an unusual set of useful properties: very high melting points (⩾ 3000 K) in combination with high thermal and electrical conductivity.

The determinative properties of nitrides are the *Me*–N and *Me*–*Me* interactions. The ratio of various contributions and the change in the nature of the chemical bond in nitrides depend mainly on the features of the electronic structure of the elements that form these compounds. The electronic structures of zirconium and nitrogen atoms can be represented as [Kr]5s^{2}4d^2 and [He]2s^{2}2p^3, respectively. The Zr–N covalent bond is due to four valence electrons of the metal atom that form directional bonds with four valence electrons of the nitrogen atoms. With an increase in the nitrogen content in zirconium nitride, the total strength of the chemical bond within the homogeneity region increases, with the Zr–N covalent bond being dominant [34, 52, 56].

Nitrides of transition metals of group IV with expanding d-shells, when interacting with nitrogen, tend to stabilize the d^5 configuration as much as possible, which leads to greater localization of valence electrons on the *Me*–*Me* bonds and a further increase in the share of this bond in the total strength of the chemical bond. With a decrease in the nitrogen content in nitrides of such metals, a redistribution of the electron density between the *Me*–N and *Me*–*Me* bonds occurs, accompanied by a change in the nature of the bond from predominantly covalent to metallic [55–58].

The ionic contribution to the chemical bond is a consequence of the difference in electronegativity between the metal and the nonmetal. As is known, nitrogen is one of the most electronegative elements, due to which the covalent bond in zirconium nitride is somewhat polarized, and the overall degree of the bond ionicity increases with increasing nitrogen content in the compound. Zirconium nitride has an electron type of conductivity throughout the homogeneity region. The high thermal and electrical conductivity of ZrN_x, characteristic of metals, is due to the ability of delocalized electrons to move through the crystal lattice. In general, nitrides of refractory metals are characterized by a covalent-metallic bond.

6. Superconductivity

Some nitrides, such as TiN, ZrN, HfN, and δNbN (all with an NaCl structure), are superconductors with transition temperatures T_c of 5.5, 10, 8.8, and 17.3 K, respectively [21]. Superconductors are materials whose electrical resistance becomes zero upon reaching a certain, so-called critical, temperature T_c. In a constant magnetic field, superconductors behave differently — there are type I and type II superconductors. It has been experimentally found that, in a cylindrical-shaped type I superconductor placed in a longitudinal magnetic field, the field is completely expelled (Meissner effect) if the field magnitude does not exceed a certain critical level H_c. In a field of higher intensity, superconductivity disappears, and the superconductor transits to the normal state. Such a transition is a first-order phase transition. Pure metals, except for niobium, in which superconductivity is observed, belong to type I superconductors.

Many alloys and nonmetallic materials — carbides, nitrides, and borides, including zirconium nitride — are type II superconductors. There are several critical magnetic fields (H_1, H_2) for type II superconductors. If the field strength H is less than H_1, the magnetic field is completely expelled from the volume of the conductor, demonstrating the complete Meissner effect. The substance is then completely in the superconducting state. If the field is such that $H_1 < H < H_2$, the field is not completely expelled from the conductor. A partial Meissner effect, or the so-called mixed state, is observed, in which the sample contains both superconducting and normal phases. It is also possible that there is another critical field H_3, such that, if the field strength $H_2 < H < H_3$, the volume of the conductor is in the normal state, and its surface layers are in the superconducting state. In a field above H_3, only the normal phase exists. Transitions of a type-II superconductor in a magnetic field from one state to another are second-order phase transitions.

For compounds of variable composition, which include ZrN_x, it was found that the transition temperature to the superconducting state T_c has a maximum value for samples with a stoichiometric composition and decreases with deviation from it [25, 59].

The authors of Ref. [59] investigated the dependence of the critical temperature T_c on the composition of ZrN_x by measuring electrical resistance using a universal four-contact method and heat capacity using a low-temperature adiabatic calorimeter. The composition of the four samples studied, according to chemical analysis data, was as follows: $ZrN_{1.01}$, $ZrN_{0.93}$, $ZrN_{0.88}$, $ZrN_{0.74}$ (or 50.2, 48.2, 46.8, 42.5 at.% of nitrogen). According to the results of electrical resistance measurements, three samples, $ZrN_{1.01}$, $ZrN_{0.93}$, and $ZrN_{0.88}$, demonstrate the phenomenon of superconductivity at temperatures of 8.5, 5.1, and 1.96 K, respectively. Heat capacity measurements were performed in the temperature range of 2–15 K for $ZrN_{1.01}$ and $ZrN_{0.93}$ and in the range of 2–10 K for $ZrN_{0.88}$ and $ZrN_{0.74}$. According to calorimetric measurements, only two samples with the maximum nitrogen

content, $ZrN_{1.01}$ and $ZrN_{0.93}$, undergo a transition to the superconducting state at temperatures of 8.9 and 6.1 K, respectively. According to the authors of [59], this circumstance can be explained by the fact that the critical temperature T_c for the sample of the $ZrN_{0.88}$ composition is lower than the temperature at which the heat capacity measurement begins. The results of measurements of the heat capacity of $ZrN_{1.01}$ and $ZrN_{0.93}$ samples in the range of 2–15 K are presented as the plot of C_p/T–T^2 in Ref. [59]. The width of the temperature range in which the transformation occurs is $\Delta T \approx 1.5-3$ K. Moreover, according to the plot, the maximum values of heat capacity for $ZrN_{1.01}$ and $ZrN_{0.93}$ samples at the transition points are approximately $C_p(8.9\ \text{K}) \approx 0.049$ J mol^{-1} K^{-1} and $C_p(6.1\ \text{K}) \approx 0.024$ J mol^{-1} K^{-1}, respectively. The authors of [59] note that, when measuring the heat capacity in a magnetic field that suppresses the transition to the superconducting state, the heat capacity curves are almost straight lines without any anomalies. As noted in [59], the superconducting transition temperature T_c depends significantly on the stoichiometry of zirconium nitride ZrN_x, as well as on the method of obtaining the sample and its preliminary temperature treatment.

In Ref. [60], the critical temperature T_c was measured in two samples prepared by two different methods (nitriding of metallic zirconium in nitrogen and nitrogen-hydrogen plasma arcs). Both ZrN samples had a stoichiometric composition: the powder density measured by the pycnometric method was close to the density determined by the X-ray diffraction method. The values of T_c obtained by measuring the electrical resistance by the four-contact method were 10.4 and 10.1 K, respectively.

In Ref. [61], the effect of tensile and shear deformation on the superconductivity of ZrN was investigated by calculation. The results show an increase in T_c to 17.1 K, which is achieved by stretching along the crystallographic axis [001].

7. Zirconium nitride low-temperature heat capacity

Low-temperature measurements of the heat capacity of zirconium nitride [62] were performed following the high-temperature ZrN enthalpy measurements in [63]. The materials used in [62] were identical to those described in [63]. Zirconium nitride ZrN was prepared from a mixture of 94.8% of zirconium nitride and 5.2% of zirconium hydride. The material was treated at 1250 °C in a nitrogen and hydrogen flow in a ratio of 3:1 until analysis showed a content of 86.65% zirconium, after which there was further heating in vacuum at 1250 °C for 14 h. According to a chemical analysis of the final product, the ZrN sample contained 86.75% zirconium, with a theoretical content of 86.69% Zr. The heat capacity measurements were performed in the temperature range of 53–298 K using a vacuum adiabatic calorimeter; the measurement error was estimated by the author at 1.7%.

Extrapolation to 0 K was performed using the empirical Debye and Einstein functions according to the equation $C_p(T) = D(360/T) + E(673/T)$. According to [62], $S^0(0-51\ \text{K}) = 1.73$ J mol^{-1} K^{-1} and $S^0(51-298.16\ \text{K}) = 37.15$ J mol^{-1} K^{-1}. Thus, the standard value of the entropy of ZrN is $S^0(298.16\ \text{K}) = 38.88 \pm 0.20$ J mol^{-1} K^{-1}.

Until recently, these were the only experimental studies of the low-temperature heat capacity of zirconium nitride. A 2009 paper [64] presents the results of measurements of the heat capacity of ZrN in the temperature range of 1.8–303 K using the high-vacuum (pressure ~ 0.01 mbar) semi-adiabatic setup PPMS-9 (Physical Property Measurement System. Quantum Design). A sample of zirconium nitride was obtained by sintering a powder (Alpha Aesar) containing 87.53 wt.% of Zr and 12.29 wt.% of N, which corresponds to the formula $ZrN_{0.9088}$. The main impurities were Hf (0.6739 wt.%) and C (0.09 wt.%); the density of the sample was 82.4% of the theoretical value. The measurement results are presented in graphical form. The authors of [64] note very good agreement between their results and low-temperature data [62]. It should be noted that the transition of ZrN to the superconducting state, previously noted in [59], was not detected in [64].

The standard values of heat capacity, entropy, and enthalpy of ZrN at 298.15 K adopted in this study were calculated according to the data from [62] and are $C_p^0(298.15\ \text{K}) = 40.42 \pm 0.20$ J mol^{-1} K^{-1}, $S^0(298.15\ \text{K}) = 38.90 \pm 0.30$ J mol^{-1} K^{-1}, and $H^0(298.15\ \text{K}) - H^0(0) = 6.590 \pm 0.03$ kJ mol^{-1}, respectively.

8. High-temperature enthalpy and heat capacity

Characterization of high-temperature dynamic properties of zirconium nitride used as an inert matrix plays a key role in assessing the performance and safety associated with the implementation of nitride fuel systems in a nuclear reactor. High-temperature measurements of the enthalpy increment of ZrN_x were performed in [63, 65–67]. The results of the measurements [67] are also reflected in books [54–56]. In all cases, the studies were carried out by the dropping method, in which enthalpy is the characteristic determined directly. To achieve an equilibrium state of the substance under study, the holding time of the sample at each measurement temperature is at least 30 min, after which the sample is dropped into a calorimeter.

The measurements of the zirconium nitride enthalpy increments in Ref. [63] were performed in the temperature range of 371–1672 K. As was said above (Section 7), the ZrN sample contained 86.75% of zirconium, which is close to the stoichiometric composition.

The high-temperature enthalpy of zirconium mononitride was investigated in [65] (533–2928 K) and [66] (523–2772 K). The sample used in [65] contained (wt.%) 86.9 of Zr, 12.8 of N, and 0.1 of Fe. In Ref. [66], the samples obtained by hot pressing, according to chemical analysis data, had a purity of 98% and contained (wt.%) 84.6 of Zr and 13.5 of N, as well as impurities (0.8 of H, 0.5 of Ca, 0.4 of Si, and 0.2 of F).

In Ref. [67], the enthalpy of zirconium mononitride in the homogeneity region was studied in the temperature range of 1200–2400 K. The authors used powders of preparations obtained by nitriding zirconium in an ammonia flow at 1170 K for 3 h with subsequent holding in purified nitrogen at 1350–1500 K (up to 4 h). X-ray analysis of the obtained samples for the compositions $ZrN_{0.72}$, $ZrN_{0.84}$, $ZrN_{0.90}$, and $ZrN_{0.96}$, carried out before and after the experiments, confirmed the single-phase nature of the preparations. The change in the mass of the samples during the experiments did not exceed 0.1%, which indicates the stability of the composition of the studied preparations. The given values of the enthalpy increments represent the average values of 6–7 measurements at each temperature.

As a result of processing their experimental data, the authors of Ref. [67] derived a generalized concentration-temperature dependence of the enthalpy of zirconium

mononitride in the homogeneity region at temperatures of 1000–2200 K, which is described by the equation

$$H^0(T) - H^0(298\ \mathrm{K}) = (1-2.705x + 3.643x^2) \times (41.885\,T + 503.672 \times 10^{-5}\,T^2 - 12971)\ [\mathrm{J\ mol^{-1}}], \quad (3)$$

where x is a variable expressing the composition of the nitride ZrN_{1-x}. The standard deviation of the experimental data from those calculated using this equation is 1.3%.

Taking into account the good agreement of their results with the data in [63], the authors of [67] calculated the main thermodynamic characteristics (heat capacity, enthalpy, entropy, and reduced thermodynamic potential) for stoichiometric ZrN ($x = 0$) in the temperature range of 298–2500 K. A comparison of the values of the enthalpy increments of stoichiometric zirconium nitride calculated by Eqn (3) at temperatures of 1200, 1600, 1900, and 2200 K with the data from [65] and [66] reveals discrepancies of (−7.4, −5.3, −3.7, −2.2%) and (−3.8, −2.7, −2.9, −3.0%), respectively, while the maximum discrepancies between the results from [67] and the reliable data from [63] do not exceed 1%. For this reason, the data from [65] and [66] were not taken into account when deriving the heat capacity equation for ZrN in the present study.

High-temperature measurements of the heat capacity of ZrN were performed in [64, 68–70] using a differential scanning calorimeter (DSC). No experimental data are presented. The results of the studies in all the listed papers are presented as equations of the temperature dependence of the heat capacity for stoichiometric ZrN.

In [68], a polycrystalline ZrN sample was prepared from powder by spark plasma sintering. X-ray analysis at room temperature showed single-phase ZrN with a cubic NaCl-type structure. The bulk density was 82% of the theoretical value. Heat capacity measurements from room temperature to 1273 K were performed in an atmosphere of high-purity argon (99.999%). The results are presented as an empirical equation for the heat capacity of ZrN in the temperature range of 400–1300 K:

$$C_\mathrm{p}(T) = 67.10 - 3.171 \times 10^{-2}\,T + 2.00 \times 10^{-5}\,T^2 - 1.505 \times 10^6\,T^{-2}\ [\mathrm{J\ mol^{-1}\ K^{-1}}]. \quad (4)$$

The heat capacity values calculated using the equation given in [68] are higher than those in the rest of the data array by $\sim 5-6\%$ over the entire measurement range.

The experimental results of measuring the heat capacity of ZrN in the temperature range of 400–1400 K, carried out in [69], are presented in the form of the equation

$$C_\mathrm{p}(T) = 45.86 + 6.82 \times 10^{-3}\,T - 5.54 \times 10^5\,T^{-2}\ [\mathrm{J\ mol^{-1}\ K^{-1}}]. \quad (5)$$

Comparing the results obtained for zirconium nitride with the literature data, the authors of [69] note the best agreement with the experimental data in Ref. [63] and those calculated in [71]. The authors of [71] proposed a method for calculating the temperature dependence of the isobaric heat capacity of titanium, zirconium, and hafnium nitrides using IR absorption spectra and elastic constants in the range of 300–1800 K. According to the authors of Ref. [71], good agreement between the calculated and experimental values allows one to reliably estimate the heat capacity of nitrides and other isostructural phases up to their melting temperatures.

The measurements of the heat capacity of zirconium nitride, performed in the same laboratory with an interval of 2 years, are presented in [70] (2007) and [64] (2009). A detailed analysis of the sample of composition $ZrN_{0.9088}$, used in both papers, is given in Ref. [64] (Section 7). The empirical equation of the temperature dependence of the heat capacity of ZrN in the range of 373–1463 K, obtained in [70], describes the experimental data with an average error of 1.15%:

$$C_\mathrm{p}(T) = 43.50 + 6.82 \times 10^{-3}\,T - 6.00 \times 10^5\,T^{-2}\ [\mathrm{J\ mol^{-1}\ K^{-1}}]. \quad (6)$$

However, at high temperatures, as noted by the authors, the calculated curve $C_\mathrm{p}(T)$ deviates from the experimental data, the maximum discrepancy being $\sim 4\%$. According to the authors of Ref. [70], such behavior of the heat capacity of zirconium nitride at high temperatures can be caused by oxidation of the sample, as evidenced by its darkening after several measurement cycles. The results of the repeated measurement [64] are also presented in the form of an equation for the temperature dependence of the ZrN heat capacity in the range of 373–1463 K:

$$C_\mathrm{p}(T) = 43.60 + 6.82 \times 10^{-3}\,T - 5.00 \times 10^5\,T^{-2}\ [\mathrm{J\ mol^{-1}\ K^{-1}}]. \quad (7)$$

A comparison of the heat capacity curves $C_\mathrm{p}(T)$, obtained in Refs [70] and [64], shows that the curves lie equidistant from each other in the entire temperature range of 373–1463 K with an insignificant discrepancy of 0.3%. At the same time, a comparison with the most reliable literary data shows that the results [70, 64] are underestimated by $\sim 5\%$.

Critical analysis of all the above-mentioned literature data indicates a significant scatter in the results of high-temperature measurements of the enthalpy and heat capacity of ZrN_x. The scatter in the thermodynamic characteristics of zirconium nitride can be due to a number of reasons, such as the stoichiometry of ZrN_x, the presence of structural defects (vacancies in the nitrogen sublattice), microstructure, porosity, the presence of impurities (mainly oxygen, carbon, hafnium), and, last but not least, the method of obtaining and preliminary heat treatment of the studied samples.

When selecting the data for deriving the equation for the heat capacity of crystalline ZrN, the quality of the samples and the characteristics of the measuring equipment were considered. The equation for the temperature dependence of the heat capacity of ZrN in the temperature range of 298.15–3970 K was obtained by joint processing of the data [63, 67, 69], with the error of all data estimated at 2%. The results of high-temperature measurements were consistent with the low-temperature data [62]:

$$C_\mathrm{p}^0(T) = 46.691 + 6.693 \times 10^{-3}\,T - 7.361 \times 10^5\,T^{-2} + 0.156 \times 10^{-6}\,T^2\ [\mathrm{J\ mol^{-1}\ K^{-1}}]. \quad (8)$$

The form of this dependence, as well as the data [64, 68–70], are shown in Fig. 3.

Worth attention are studies of the heat capacity of mixed nitrides $(Pu_{0.25}Zr_{0.75})N$ [69] and $(Zr_{0.78}Pu_{0.22})N$ [64], which are of interest in the context of using nitride fuel, in which ZrN serves as an inert matrix. In Ref. [69], the measurements of the heat capacity of $(Pu_{0.25}Zr_{0.75})N$ in the range of 400–1400 K were performed using a differential scanning calorimeter (DSC 404 NETZSCH). The measurement error

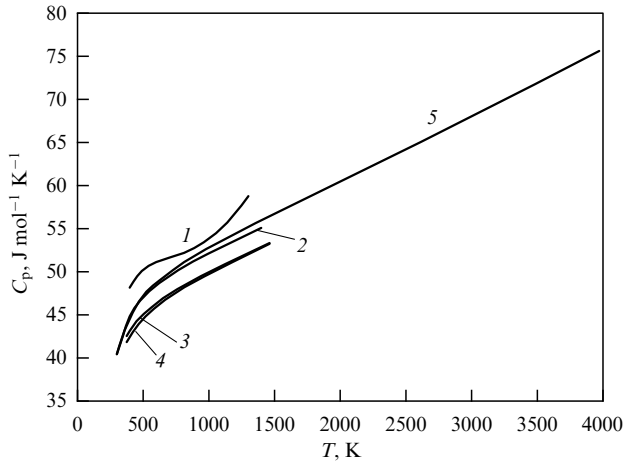

Figure 3. Dependence of zirconium nitride heat capacity on temperature: *1* — [68]; *2* — [69]; *3* — [70]; *4* — [64]; *5* — the present study, Eqn (8).

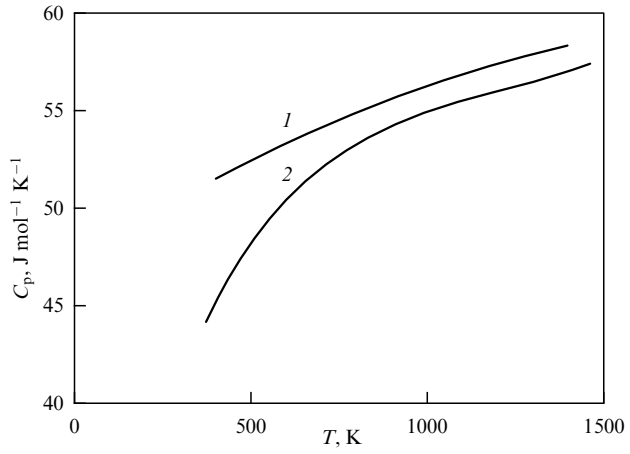

Figure 4. Temperature dependence of heat capacity for mixed nitrides: *1* — $(Pu_{0.25}Zr_{0.75})N$ [69]; *2* — $(Zr_{0.78}Pu_{0.22})N$ [64].

was estimated by the authors at ~ 5%. The experimental data obtained were approximated by the equation

$$C_p(T) = 47.24 + 1.18 \times 10^{-2}\, T - 2.78 \times 10^{-6}\, T^2 \ [\text{J mol}^{-1}\ \text{K}^{-1}]. \quad (9)$$

The results of high-temperature measurements of the heat capacity of $(Zr_{0.78}Pu_{0.22})N$, performed using a semi-adiabatic DSC in the temperature range of 373–1463 K [64], are presented by the equation

$$C_p(T) = 33.83 + 4.75 \times 10^{-2}\, T - 4.00 \times 10^{5}\, T^{-2} - 3.60 \times 10^{-5}\, T^2 + 1.00 \times 10^{-8}\, T^3 \ [\text{J mol}^{-1}\ \text{K}^{-1}]. \quad (10)$$

The measurement error, according to the authors' estimate [64], was 3%.

The curves of the temperature dependence of the heat capacity $C_p(T)$ of mixed nitrides are shown in Fig. 4.

9. Liquid zirconium nitride heat capacity

Until recently, the thermodynamic properties of liquid zirconium nitride had not been considered in the literature. The heat capacity of stoichiometric liquid ZrN was estimated in the reference books [72] (66.944 J mol^{-1} K^{-1}), [73] (66.944 J mol^{-1} K^{-1}), and [74] (58.576 J mol^{-1} K^{-1}). The estimated enthalpies of melting at the recommended melting temperatures (3253, 3253, and 3225 K) were 83.68, 83.68, and 67.362 kJ mol^{-1}, respectively.

An attempt to study the melting process and the heat capacity of the liquid phase of ZrN was made in Ref. [75]. The authors used the pulsed electric current heating method [76], which makes it possible to measure the bulk properties of a substance (electrical resistance, enthalpy, and heat capacity). Zirconium nitride samples were deposited in the form of a thin layer (2.5 μm) on insulating substrates (K-8 glass) using magnetron sputtering. Pulsed current heating ensured that the nitride reached the melting region within 5 μs. The same authors subsequently used the method under consideration to study comparatively massive sintered zirconium nitride samples [77] containing about 10 mol.% tetragonal zirconium dioxide, i.e., a large amount of oxygen impurity. Given the lack of other data, we will consider the results of these studies in more detail. Figure 5a shows a view of ZrN coating deposited on a K-8 glass plate [75]. A typical view of a glass cell with a glued-in sintered sample (plate) is shown in Fig. 5b.

Figure 6 shows a typical form of oscillograms obtained in an experiment on pulsed heating of a sintered ZrN sample [77].

The results of processing oscillograms for one such rapid heating of zirconium nitride are presented below (see Figs 8, 9).

In Refs [75, 77], the temperature of the samples was measured using a high-speed brightness pyrometer, which was calibrated using a temperature lamp. The temperature of the samples was calculated in [78] using Planck's formula for blackbody radiation and literature data on the spectral emissive capacity of zirconium nitride, which resulted in the dependence $T(t_i)$. Measurements of the current through the sample and the voltage drop across the sample were performed using a digital oscilloscope.

The Joule heating energy dissipated in the sample was calculated using the formula [79]

$$E(t) = \frac{1}{m}\int_0^t I(t)\, U(t)\, \mathrm{d}t \approx \frac{1}{m}\sum_0^k I(t_i)\, U(t_i)\, \tau, \quad (11)$$

where m is the sample mass; t is the current time, a multiple of τ, where τ is the digital oscilloscope sampling period; t_1 is the ith moment of time from the start of the sweep; $U(t_i) = u(t_i) - L(I(t_{i+1}) - I(t_i))/\tau$ is the voltage drop across the active resistance of the sample; $u(t_i)$ is the voltage drop on the sample; and L is inductance of the sample.

The heat capacity of the samples was calculated, ignoring small heat losses (less than 1% for massive samples) according to the formula [79]

$$C_p = \frac{E\left(T(t_i + n\tau)\right) - E\left(T(t_i)\right)}{T(t_i + n\tau) - T(t_i)}, \quad (12)$$

where $E(T)$ is the Joule heating energy (11); t_i, $(t_i + n\tau)$ is the beginning and end of the i-th time interval; and n is the number of points in the specified time interval. The obtained value of C_p was related to the average temperature of the interval $T_{\text{ref}} = [T(t_i + n\tau) + T(t_i)]/2$.

The elemental composition of the samples in [75, 77] was approximately the same: N/Zr = 1.33 and 1.36, the oxygen content being 10.76 and 7.25 at.%. The nonmetal/Zr ratio was greater than the N/Zr ratio. The density was 6.7 and

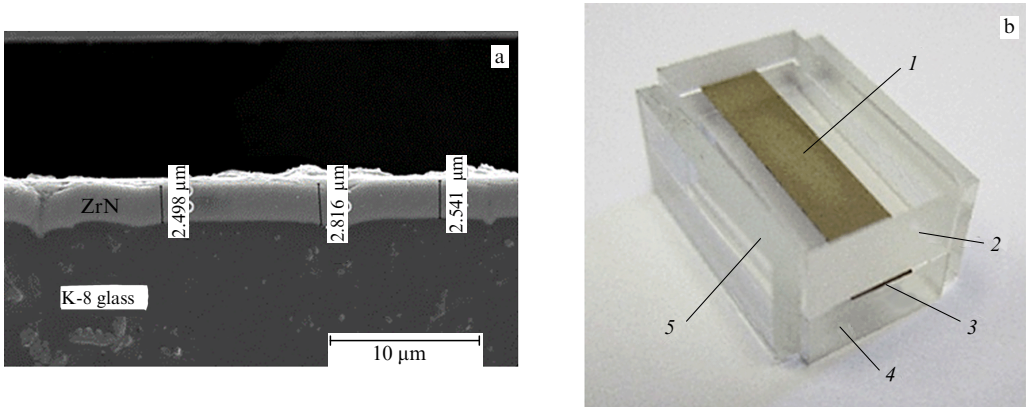

Figure 5. (a) Side surface of plate of K-8 glass with ZrN coating. Coating thickness is indicated [75]. (b) One of the glass cells with a sample of sintered ZrN: *1* — ZrN sample; *2*, *4* — glass plates; *3* — nitride plate edge (from both sides); *5* — side glass plates.

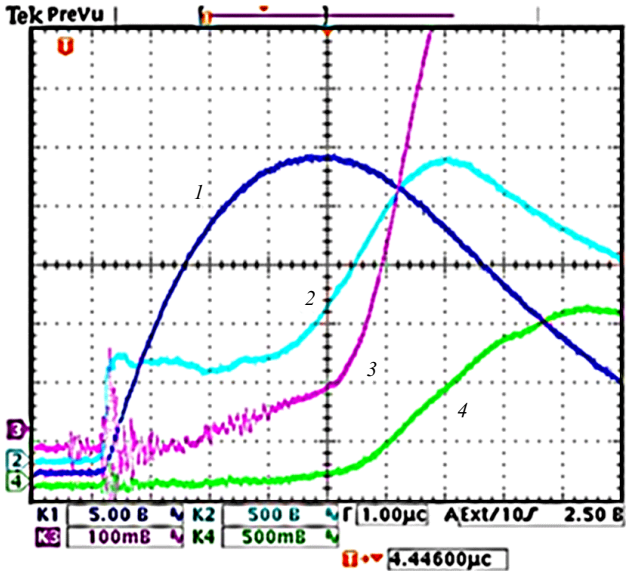

Figure 6. Oscillograms of the process of ZrN sample heating by a pulse of current (scan 10 μs): *1* — current pulse; *2* — voltage applied to sample; *3*, *4* — pyrometer signal at high and low sensitivity. Kink in oscillograms *3*, *4* corresponds to origin of sample liquid phase [77].

6.9 g cm^{-3}, respectively. The density of the ZrN coating was estimated by the mass of the deposited layer on the witness sample. For comparison, the density of pure ZrN according to [80] is 7.09 g cm^{-3}, while according to [31] the X-ray density is 7.32 g cm^{-3}.

It should be noted here that, unlike zirconium carbide, the nitride lattice can have not only nonmetal (nitrogen) vacancies, but also metal vacancies, i.e., the N/Zr ratio can be either less than or greater than 1, depending on which sublattice — metal or nonmetal — has more vacancies [31]. In these samples, the number of vacancies in the zirconium sublattice was greater than in the nitrogen sublattice.

The microstructure of the film samples (Fig. 7a) differed from that of the bulk samples (Fig. 7b). The surface of the ZrN coating (Fig. 7a) consisted of blocks with dimensions of 0.2–0.5 μm, between which developed slit-like pores were visible. The fracture of the sintered ZrN sample (Fig. 7b) was predominantly transcrystalline in nature with characteristic cleavage steps on the grains of the base material, the linear dimensions of which were $\sim$ 10 μm.

The difference in microstructure resulted in significant differences in the specific electrical resistance (related to the initial dimensions of the sample): in [75] it was 900 μΩ cm near the melting point and in [77] it was 130 μΩ cm.

According to [75, 77], zirconium nitride melted at 2700 K (in [77] in the temperature range of 2600–2700 K), which is significantly lower than the T_m values given in other experimental studies (3200–3970 K depending on the nitrogen pressure (see Section 3)). The authors of [75, 77] explained such a low melting point by the presence of a large amount of oxygen in both cases (4.05 and 2.6 wt. %, respectively). It is known that an oxygen impurity in an amount of 0.5–1 wt. % reduces the melting point of zirconium nitride by 200–300 K [42]. It can be assumed that the higher content of this impurity in [75, 77] led to a greater decrease in the melting point of ZrN (by 500 K or more). The effect of the superstoichiometric composition of the samples on the melting point cannot be ruled out either.

The temperature dependences of the specific heat capacity [75, 77] are plotted in the temperature ranges of 2000–3200 K and 2300–4500 K, respectively. In [75], the specific heat capacity of liquid ZrN was approximately constant, and it was $C_p = 140 \pm 70$ J mol^{-1} K^{-1} in the temperature range of 3000–3200 K. The large error in these measurements is caused by the high error in determining the mass of the sample (errors in measuring the density and measuring the thickness of the film sample). Figure 8 shows the specific heat capacity of sintered ZrN, obtained in experiment [77].

In [77], the specific heat capacity of the solid phase was not measured, and the liquid phase C_p (curve *3* in Fig. 8) decreases after melting and then remains almost constant in the temperature range of 2900–3700 K with an average value of 84 ± 25 J mol^{-1} K^{-1}. Then, it increases almost linearly to 116 ± 35 J mol^{-1} K^{-1} with an increase in temperature to 4000 K, which is possibly due to the sample approaching the boiling point. For sprayed samples, the measurement error is significantly higher than for sintered ones. Due to much smaller uncertainties, preference should be given to the data from [77]. Note that the result in [77], 84 ± 25 J mol^{-1} K^{-1}, is close to estimates [72, 73].

Figure 9 [77] shows the result of measuring the temperature dependence of the specific electrical resistance of the nitride $0.9ZrN + 0.1ZrO_2$. The studied range of 2300–4500 K is divided by the break points of curve *1* into three regions: the solid phase (up to 2600 K); the melting region of 2600–2700 K;

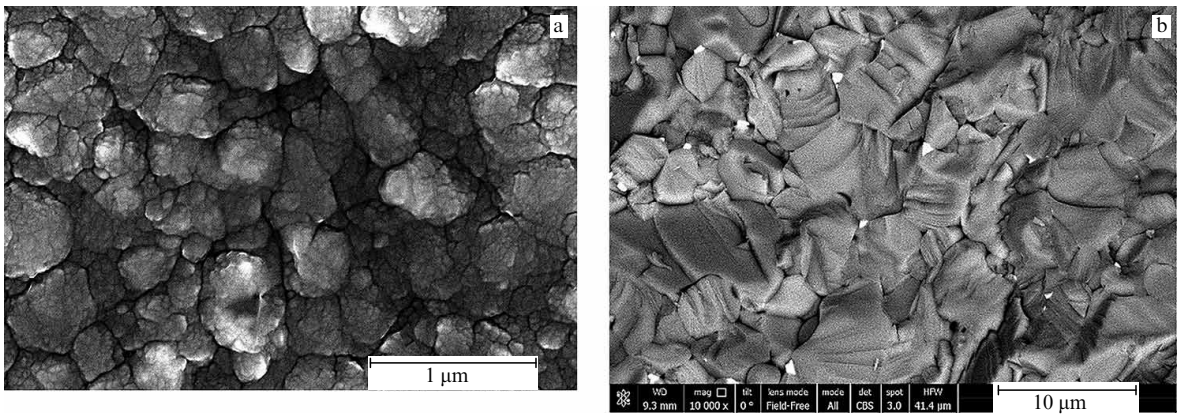

Figure 7. (a) Surface microstructure of ZrN coating 2.5 μm thick. (b) Microstructure of the sintered ZrN sample kink. Light areas are enriched with tungsten.

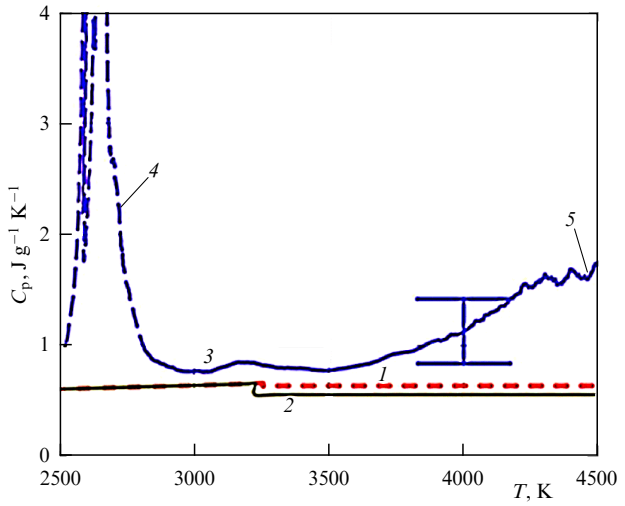

Figure 8. Temperature dependence of C_p of the liquid sample $0.9ZrN + 0.1ZrO_2$: *1* — data for ZrN [72, 73]; *2* — data for ZrN [74]; *3* — data from [77]. The dashed part of curve *3* is presented for illustration only; *4* — melting region; *5* — hypothetical boiling [77].

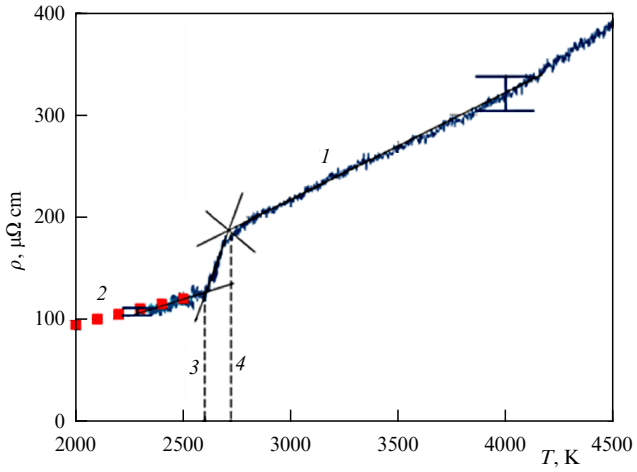

Figure 9. Temperature dependence of specific electric resistance (related to initial dimensions of the sample) for $0.9ZrN + 0.1ZrO_2$: *1* — data from [77]; *2* — red squares — data for ZrN obtained by the steady-state method [84]; *3* — melting beginning; *4* — end of melting and beginning of liquid phase [77].

and the region of the liquid phase, in which the electrical resistance increases almost linearly. In the temperature range of 2700–4200 K, this dependence has the form $\rho = 183 + 0.106(T-2700)$ (μΩ cm).

Note the good agreement between the results of measuring the specific electrical resistance of ZrN in the solid state during pulsed and steady-state heating. However, the melting temperature (region *3–4* in Fig. 9) is underestimated due to the significant oxygen content in the original samples.

It follows from the above that the melting process and thermodynamic properties of the liquid phase of zirconium nitride require further careful study using samples with a minimum content of impurities (especially oxygen). A convenient — and practically the only — method for such studies is heating with a current pulse of microsecond duration [76]. In such a short time, all types of heat loss are less than 1–2%, which allows them to be ignored and the specific heat capacity of the sintered sample to be directly measured. The method is used to study metals [81], as well as graphite [82] and conductive ceramics [83], to temperatures of 5000–8000 K. In the latter case, as experiments show, it is possible to heat brittle samples of carbides, as well as the zirconium nitride under consideration, until melting without destruction.

Let us note the main important advantages of studying conductive substances with rapid (microsecond) heating by current:

(1) The sample has a constant cross section (foil or wire). This ensures the equality of the current density, and therefore the temperature, at all points of the sample, which allows reliable measurement of the temperature, in particular, when using the black body model (when the emissive capacity of the material is unknown).

(2) Due to the short duration of the process, the shape of the sample remains unchanged during the experiment (due to the inertia of the mass), while thermal expansion is not limited: the speed of sound in the material ensures normal thermal expansion during the experiment. For example, in the experiment, the boiling of hafnium was observed at a temperature of about 4900 K [81] (in the form of a piece of wire) with both the shape of the cylinder and its position in space remaining unchanged.

(3) To conduct the experiment, it is sufficient to use a small amount of material. For example, in [83], data are presented on the study of the properties of a plate of mixed carbide (TaC + HfC) with a thickness of 1 μm up to 5000 K. This property of the method is advantageous, for example, in the study of precious metals.

10. Zirconium nitride in modern technologies

Below is a brief illustrative list of works demonstrating the continuing interest in zirconium nitride — a substance that finds application in a wide variety of fields of science and technology. The use of ZrN in nuclear technology was mentioned above. Review [85] examines modern thermal protection systems for aircraft and summarizes the achievements of Russian and foreign science in the field of developing carbon-ceramic composite materials, "...the components of which are super-refractory borides, carbides and nitrides of transition metals of group IV (ZrB_2, HfB_2, ZrC, HfC, ZrN, HfN)" [85]. Review [85], in general, is aimed at studying methods for providing thermal protection for aircraft under high-temperature conditions in the presence of thermal and chemical processes in the gas flow and in the protective coating itself.

Zirconium nitride has a relatively simple NaCl-type lattice, which can be represented as two face-centered cubic lattices consisting of zirconium and nitrogen atoms, nested one inside the other and shifted relative to each other by half a period. The simplicity of this lattice allows studying the properties of ZrN and materials based on it using computational methods [86], as well as investigating the possible existence of a whole set of stable and metastable nitride phases of zirconium of different stoichiometries using computer modeling [87].

The set of unique properties of ZrN (thermal, electrical, radiative, etc.) finds application in promising solar energy systems [88] and fuel cells [90]. Analyses of the superconducting properties of ZrN are used to create new superconducting materials [90]. A large number of papers are devoted to the description of various methods for obtaining and studying the properties of nitride films [91].

11. Conclusion

The combination of nuclear-physical, thermal, and mechanical properties makes zirconium nitride a promising material for nuclear power engineering, in particular, as an inert matrix material in the development of fuels for various types of reactors. Zirconium nitride is used in aircraft and rocket engineering as one of the components of composite heat-shielding materials. Zirconium nitride is also known to be used in other high-temperature technologies. All this requires obtaining reliable data on the thermophysical properties of zirconium nitride in the widest possible temperature range.

Based on a critical analysis and numerical processing of experimental data on the high-temperature enthalpy and heat capacity of zirconium nitride available in the literature, an equation for the temperature dependence of the heat capacity of solid ZrN in the temperature range of 298.15–3970 K was obtained:

$$C_p^0(T) = 46.691 + 6.693\times10^{-3}\,T - 7.361 \times 10^5\,T^{-2} + 0.156\times10^{-6}\,T^2\ [\text{J mol}^{-1}\ \text{K}^{-1}].$$

Based on the analysis of available literature data on the nature and melting point of zirconium nitride of various compositions and at various nitrogen pressures, the temperature of congruent melting of ZrN_x was selected. When choosing the temperature and stoichiometry of the ZrN_x composition corresponding to the congruent nature of melting, preference was given to the value $T_m = 3970 \pm 70$ K with a composition of $ZrN_{0.98}$ and a nitrogen pressure of 60 atm.

To obtain the most accurate value of the enthalpy of ZrN_x formation in the homogeneity region, calorimetric measurement data and estimates of this value by various calculation methods were used. As a result of the analysis of the entire set of data presented, the value $\Delta_f H^0(298.15\ \text{K}) = -366.6 \pm 1.5$ kJ mol^{-1} can be recommended for stoichiometric ZrN.

The liquid phase of zirconium nitride had not been studied until recently. For the first time, the properties of the liquid phase of zirconium nitride were investigated by the method of rapid microsecond heating with a current pulse up to 4000 K. Samples of nitride with an oxygen content of ~ 10 at.% were investigated in the form of a film coating 2.5 μm thick and in the form of sintered ceramics 140 μm thick. According to preliminary estimates, the high content of oxygen impurities led to a decrease in the melting point of the nitride to 2700 K.

The heat capacity of the liquid phase of zirconium nitride (composition $0.9ZrN+0.1ZrO_2$) at temperatures of 2900–3700 K is constant and equal to $C_p = 84 \pm 25$ J mol^{-1} K^{-1}, which is close to the estimates obtained earlier in several reference books. The specific electrical resistance of the liquid phase of zirconium nitride of the same composition in the temperature range of 2700–4200 K changes linearly: $\rho = 183 + 0.106 \times (T - 2700)$ [μΩ cm].

In this paper, it is shown that the method of heating with a microsecond current pulse allows studying zirconium nitride and other superdense substances on comparatively massive and thin sprayed samples. This method is most suitable for studying the properties of the solid phase near melting and the melting region of the liquid phase of refractory and super-refractory conducting substances.

Acknowledgments. N M Aristova carried out the work within the framework of the State Assignment to the Joint Institute for High Temperatures of the Russian Academy of Sciences for 2024 no. 075-00270-24-00 of 27.12.2023. S V Onufriev and A I Savvatimskiy are grateful to the Russian Science Foundation (grant no. 19-79-30086P, Lebedev Physical Institute, head academician: G A Mesyats).

References

1. US D.O.E. and the Generation IV International Forum. A Technology Roadmap for Generation IV Nuclear Energy Systems. US-DOE (2002)
2. Ronchi C et al., in *Proc. of the GLOBAL 2005. No. 391. Tsukuba Japan. October 9–13, 2005*
3. Rondinella V V et al., in *Proc. of the ANS Winter Conf., Washington DC, USA, Transaction ANS 97, November 11–15, 2007*
4. Ronki K *High Temp.* **45** 552 (2007); *Teplofiz. Vys. Temp.* **45** 609 (2007)
5. Rogozkin B D, Stepennova N M, Proshkin A A *Atom. Energy* **95** 624 (2003); *Atom. Energ.* **95** (3) 208 (2003)
6. Alekseev S V, Zaitsev V A *Nitridnoe Toplivo dlya Yadernoi Energetiki* (Nitride Fuel for Nuclear Power Engineering) (Moscow: Tekhnosfera, 2013) p. 239
7. Merja Pukari "Experimental and theoretical studies of nitride fuel," Doctoral PHD Dissertation (Stockholm, Sweden: KTH Royal Institute of Technology, 2013)
8. Bondarenko G G et al. *Metally* **6** 59 (2011)
9. Ivanov A S et al. *Voprosy Atom. Nauki Tekh. Ser. Fiz. Yad. Reaktorov* (2) 106 (2015)
10. Rusinkevich A A et al. *Voprosy Atom. Nauki Tekh. Ser. Fiz. Yad. Reaktorov* (2) 114 (2015)
11. Ivanov A S "Corrosion of steel claddings of fast reactors fuel elements in the interaction with uranium-plutonium nitride fuel,"

in *Technical Meeting on Structural Materials for Heavy Liquid Metal Cooled Fast Reactors, IAEA Headquarters Vienna, Austria 15–17 October* (Vienna: IAEA Headquarters, 2019)
12. Ivanov A S, Rusinkevich A A, Rusinkevich V A *Voprosy Atom. Nauki Tekh. Ser. Fiz. Yad. Reaktorov* (1) 48 (2021)
13. Arai Y, Morihra M, Ohmichi T *J. Nucl. Mater.* **202** 70 (1993)
14. Streit M et al. *J. Nucl. Mater.* **319** 51 (2003)
15. Ryu H J et al. *J. Nucl. Mater.* **352** 341 (2006)
16. Domagala R F, McPherson D J, Hansen M *J. Metals* **8** 98 (1956)
17. Smagina E I, Kutsev V S, Ormont B F *Problemy Fiz. Khim.* **2** 118 (1959)
18. Smagina E I, Kutsev V S, Ormont B F *Zh. Fiz. Khim.* **24** 2328 (1960)
19. Samsonov G V, Verkhoglyadova T S *Dokl. Akad. Nauk USSR* (1) 48 (1962)
20. Kaufman L, Bernstein H *Computer Calculation of Phase Diagrams with Special Reference to Refractory Metals* (New York: Academic Press, 1970)
21. Toth L E *Transition Metal Carbides and Nitrides* (New York: Academic Press, 1971)
22. Storms E K "Phase relationships and electrical properties of refractory carbides and nitrides," in *Solid State Chemistry* Vol. 10 (Ed. L E Roberts) (Baltimore, MD: Univ. Park Press, 1972)
23. Eronyan M A, Avarbe R G *Izv. Akad. Nauk SSSR Neorg. Mater.* **10** 2156 (1974)
24. Kubaschewski O *Zirconium: Physico-Chemical Properties of Compounds and Alloys* (Atomic Energy Review, Special Issue No. 6) (Vienna: International Atomic Energy Agency, 1976)
25. Christensen A Norlund, Fregerslev S *Acta Chem. Scandinavica A* **31** 861 (1977)
26. Moffatt W G *The Handbook of Binary Phase Diagrams* (Schenectady, NY: Genum Publ. Corp., 1984)
27. Massalski T B *Binary Alloy Phase Diagrams* 2nd ed. (Metals Parks, OH: ASM Intern., 1990)
28. Gribaudo L, Arias D, Abriata J *J. Phase Equilibria* **15** 441 (1994)
29. Ogava T *J. Alloys Compd.* **203** 221 (1994)
30. Wang W E, Olander D R *J. Alloys Compd.* **224** 153 (1995)
31. Pierson H O *Handbook of Refractory Carbides and Nitrides. Properties, Characteristics, Processing and Applications* (Westwood, NJ: Noyes Publ., 1996)
32. Ma X et al. *J. Alloys Compd.* **373** 194 (2004)
33. Lengauer W *Transition Metal Carbides, Nitrides and Carbonitrides* (Weinheiin: Wiley-VCH Verlag GmbH, 2008)
34. Harrison R W, Lee W E *Adv. Appl. Ceramics* **115** (5) 294 (206)
35. Sridar S, Kumar R, Hari Kumar K C *Calphad Comput. Coupling Phase Diagrams Thermochem.* **56** 102 (2017)
36. NIST Standard Reference Database 31. The Phase Equilibria Diagrams PC Database, Version 4.5 (2021)
37. Friederick E, Sittig L *Z. Anorg. Allg. Chem.* **143** 293 (1925)
38. Agte C, Moers K *Z. Anorg. Allg. Chem.* **198** 233 (1931)
39. Yanchur V P et al. *Izv. Akad. Nauk SSSR Neorg. Mater.* **5** 1012 (1969)
40. Eronyan M A, Avarbe R G, Nikol'skaya T A *Zh. Prikl. Khim.* **46** 428 (1973)
41. Ettmayer P, Kieffer R, Hattinger F *Metall.* **28** 1151 (1974)
42. Eronyan M A, Avarbe R G, Nikol'skaya T A *Izv. Akad. Nauk SSSR Neorg. Mater.* **12** (2) 247 (1976)
43. Neuman B, Kroger C, Kunz H *Z. Anorg. Allg. Chem.* **218** 379 (1934)
44. Mah A D, Gellert N L *J. Am. Chem. Soc.* **78** 3261 (1956)
45. Humphrey G L *J. Am. Chem. Soc.* **76** 978 (1954)
46. Hoch M, Dingledy D P, Johnston H L *J. Am. Chem. Soc.* **77** 304 (1955)
47. Apin A Ya, Lebedev Yu A, Nefedova O I *Zh. Fiz. Khim.* **32** 819 (1958)
48. Smagina E I, Kutsev V S, Ormont B F *Dokl. Akad. Nauk SSSR* **115** (2) 354 (1957)
49. Gal'braikh E I et al. *Poroshk. Metallurg.* (9) 62 (1970)
50. Kornilov A N, Ushakova I M, Skuratov S M *Zh. Fiz. Khim.* **41** (1) 200 (1967)
51. Mulokozi A M *J. Less Common Met.* **79** 139 (1981)
52. Samsonov G V *Nitridy 1* (Nitrides 1) (Kiev: Naukova Dumka)
53. Geld P V, in *Transition Metal Carbides and Nitrides* (Ed. L E Toth) (New York: Academic Press, 1971); Translated into Russian: *Karbidy i Nitridy Perekhodnykh Metallov* (Ed. L Toth) (Moscow: Mir, 1974) p. 264
54. Litvinenko V F et al., in *Elektronnoe Stroenie i Fiziko-Khimicheskie Svoistva Splavov i Soedinenii na Osnove Perekhodnykh Metallov* (Electronic Structure and Physico-Chemical Properties of Alloys and Compounds Based on Transient Metals) (Exec. Ed. G V Samsonov) (Kiev: Naukova Dumka, 1976) p. 168
55. Bolgar A S, Litvinenko V F, Timofeeva I I, in *Konfiguratsionnye Predstavleniya Elektronnogo Stroeniya v Fizicheskom Materialovedenii* (Configuration Representations of Electronic Structure in Physical Materials Science) (Exec. Ed. Ya I Dutchak) (Kiev: Naukova Dumka, 1977) p. 116
56. Bolgar A S, Litvinenko V F *Termodinamicheskie Svoistva Nitridov* (Thermodynamical Properties of Nitrides) (Kiev: Naukova Dumka, 1980) p. 281
57. Fernández Guillermet A, Hüglund J, Grimvall G *Phys. Rev. B* **45** 11557 (1992)
58. Balasubramanian K, Khare S V, Gall D *Acta Mater.* **152** 175 (2018)
59. Lovchinov V A et al. *Phys. Scr.* **27** (3) 207 (1983)
60. Konuma M, Matsumoto O *J. Less Common Met.* **56** 129 (1977)
61. Weixue L et al. *J. Phys. Chem. Lett.* **12** 1985 (2021)
62. Todd S S *J. Am. Chem. Soc.* **72** 2914 (1950)
63. Coughlin J P, King E G *J. Am. Chem. Soc.* **72** 2262 (1950)
64. Ciriello A et al. *J. Alloys Compd.* **473** 265 (2009)
65. Neel D S, Oglesby S, Pears C D, WADD Technical Documentary Report No. 60-924 (Birmingham, AL: Southen Research Institute, 1962) p. 89
66. Hedge J C et al. "Thermal properties of refractory alloys," US Air Force Report ASD-TDR 63-597, 1-128 (1963)
67. Bolgar A S et al. *Poroshk. Metallurg.* (11) 48 (1976)
68. Adachi J et al. *J. Alloys Compd.* **399** 242 (2005)
69. Basini V et al. *J. Nucl. Mater.* **344** 186 (2005)
70. Ciriello A et al. *J. Nucl. Mater.* **371** 129 (2007)
71. Kogel' S P et al. *Neorg. Mater.* **19** 1665 (1983)
72. Kelley K K, U.S. Bureau of Mines Bull. No. 584 (Washington, DC: U.S. Govt. Print. Off., 1960)
73. Schick H L *Thermodynamics of Certain Refractory Compounds* (New York: Academic Press, 1966)
74. Chase M W (Jr.) (Ed.) "NIST-JANAF thermochemical tables, fourth edition, Pt. I, II" *J. Phys. Chem. Ref. Data.* (1998) Monograph 9
75. Onufriev S V et al. *High Temp.* **53** 455 (2015); *Teplofiz. Vys. Temp.* **53** 478 (2015)
76. Savvatimskiy A I, Onufriev S V *Phys. Atom. Nucl.* **79** 1637 (2016); *Yad. Fiz. Inzh.* **6** 622 (2015) https://doi.org/10.1134/S1063778816140131
77. Onufriev S V, Savvatimskiy A I, Muboyadzhyan S A *Mater. Res. Express* **6** 125554 (2019) https://doi.org/10.1088/2053-1591/ab6e39
78. Onufriev S V *Bull. Russ. Acad. Sci. Phys.* **82** 372 (2018); *Izv. Ross. Akad. Nauk Ser. Fiz.* **82** 430 (2018) https://doi.org/10.3103/S1062873818040147
79. Onufriev S V, Savvatimskiy A I *High Temp.* **56** 678 (2018); *Teplofiz. Vys. Temp.* **56** 704 (2018)
80. Grigoriev I S, Meilikhov E Z (Eds) *Handbook of Physical Quantities* (Boca Raton, FL: CRC Press, 1997); Translated from Russian: *Fizicheskie Velichiny. Spravochnik* (Moscow: Energoatomizdat, 1991)
81. Savvatimskiy A I, Korobenko V N *Vysokotemperaturnye Svoistva Metallov Atomnoi Energetiki* (*Tsirkonii, Gafnii i Zhelezo pri Plavlenii i v Zhidkom Sostoyanii*) (High-Temperature Properties of Metals of Nuclear Power Engineering (Zirconium, Hafnium and Iron During Melting and in Liquid State)) (Moscow: Izd. Dom MEI, 2012)
82. Savvatimskiy A I, Onufriev S V *Phys. Usp.* **63** 1015 (2020); *Usp. Fiz. Nauk* **190** 1085 (2020)
83. Savvatimskiy A I, Onufriev S V, Aristova N M *Phys. Usp.* **65** 597 (2022); *Usp. Fiz. Nauk* **192** 642 (2022)
84. Petrova I I et al. *Teplofiz. Vys. Temp.* **10** 1007 (1972)
85. Astapov A N et al. *High Temp.* **59** 221 (2021); *Teplofiz. Vys. Temp.* **59** 248 (2021)
86. Mohamed Sheik Sirajuddeena M, Shameem Banu I B *AIP Adv.* **4** 057121 (2014)
87. Yu S et al. *RSC Adv.* **7** 4697 (2017)
88. Ijaz S et al. *Opt. Express* **29** 31537 (2021)
89. Liu H et al. *Chem. Sci.* **14** 9000 (2023)
90. Liao Z-W et al. *Phys. Rev. B* **108** 014501 (2023)
91. Carvalho P et al. *J. Appl. Phys.* **103** 104907 (2008)